2012 IEEE/RSJ International Conference on Intelligent Robots and Systems
October 7-12, 2012. Vilamoura, Algarve, Portugal

Force sensing using artificial magnetic cilia

Antti Virta, Jaakko V.I. Timonen, Robin H.A. Ras and Quan Zhou, *Member, IEEE.*

Abstract— **This paper proposes a sensing concept based on measuring the geometrical deformation of artificial magnetic cilia indirectly with a magnetoresistive sensor. The cilia are fabricated with a template-free method based on the evaporation of solvent from a suspension containing micron-sized magnetic particles and dissolved elastomeric polymers under constant magnetic field. The sensing concept has applications in e.g. flow measurement and tactile force sensing. A mathematical model for the magnetic field of the cilium is developed and experimental results are presented to verify the model.**

I. INTRODUCTION

Cilia are thin, hair-like organelles present on the apical surface of most mammalian cells. Cilia serve multiple purposes in a cell, including fluid shear stress sensing, cell cycle regulation and cell signalling [1]. Cilium-like structures appear also elsewhere on biological organisms. Crickets, for example, evade predators by using arrays of microscopic hair located in the rear-most part of their body to sense airflows around them. Fish use their lateral line, which consists of cells with cilium-like organelles, to sense the movement and tiny vibrations of water around them [2].

Cilia have inspired many biomimetic actuator and sensor designs. Artificial magnetic cilia comprised of ferromagnetic elastomer composite [3] and superparamegnetic beads [4] have been used as microfluidic actuators for flow generation. Motion of the cilia is generated with a varying magnetic field supported by the fact that the cilia will align themselves with the magnetic field due to their magnetization.

Artificial cilia sensors have been employed in flow measurement, flow pattern recognition and vibration detection. Cilia have been fabricated using multiple-step micromachining techniques [5]–[8] and recently with thermo-direct drawing of piezoelectric polymer [9]. Sensing principle is based on either capacitive [5], [7] or piezoelectric sensing elements [6], [8], [9] that are deposited as a part of the cilia manufacturing process. The major drawback of the aforementioned fabrication methods is their complexity, as several steps and special equipment are required to complete the manufacturing process.

Manuscript received March 9, 2012. This work was supported by the Finnish Academy of Sciences under grant 134206 Programmable and Spatially Multi-scale Self-assembly of Microcomponents, MUSA (2010-2013).

A. Virta and Q. Zhou are with the Department of Automation and Systems Technology, School of Electrical Engineering, Aalto University, P.O Box 15500, 00076 Aalto, Finland. antti.virta@aalto.fi; quan.zhou@aalto.fi

Jaakko V.I. Timonen and Robin H.A. Ras are with the Department of Applied Physics, School of Science, Aalto University, P.O Box 15100, 00076 Aalto, Finland. jaakko.timonen@aalto.fi; robin.ras@aalto.fi

In this paper, we propose a force sensing concept based on easy to fabricate, low-cost artificial magnetic cilia. The cilia are fabricated with a template-free method based on the evaporation of solvent from a suspension containing microscopic ferromagnetic cobalt particles and dissolved elastomeric polymer under magnetic field [10]. The sensing concept is based on the estimation of the geometric deformation of the cilium by measuring its magnetic field. In order to achieve this, a gray-box model utilizing a set of spatially distributed dipoles is derived to characterize the magnetic field of the cilium. The parameters of the model are estimated based on experimental measurements of the magnetic field of the cilium.

The paper is organized as follows. In the following section, the sensing concept and the fabrication process of the cilia are discussed. In third section, a magnetic field model for a single cilium is derived. The fourth section provides experimental results and sensitivity analysis of the proposed model to parameter variations. Section five discusses the results and concludes the paper.

II. DESIGN AND FABRICATION

A. *Sensing concept*

Cilia fabricated as described in [10] are composed of ferromagnetic cobalt particles and elastomeric polymer which binds the cobalt particles together. The ferromagnetic particles give cilia magnetic field that can be used to measure external forces acting on the cilia.

An external force will result in deformation of a cilium. If the model for the magnetic field of the cilium is known, this deformation can be estimated by measuring the magnetic field of the cilium in a fixed point outside the cilium with a magnetic field sensor. This scheme can be utilized to measure various external forces, as illustrated in fig. 1.

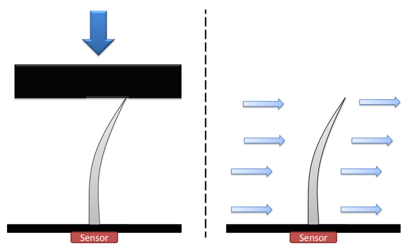

Fig. 1. Sensing principles of the proposed cilium sensor in tactile and flow measurements. A single cilium is placed on top of a magnetic field sensor. The cilium bends due to an external force caused by e.g. a tactile interaction or fluid flow. The resulting change in the magnetic field is detected by the sensor.

978-1-4673-1736-8/12/$31.00 ©2012 IEEE

The sensitivity of the proposed sensing scheme is limited by the resolution of magnetic field sensor used. In order to maximize the sensor resolution, the distance between the sensing element and the cilium should be minimized. Alternatively, increasing the magnetic mass, i.e. placing multiple cilia on a row formation perpendicular to the sensitive axis of the sensor, increase the sensitivity. However, in this paper only a single cilium configuration is examined and multiple cilia configurations remain as further work.

B. Fabrication of the magnetic cilia

Fabrication process has multiple parameters that affect the physical properties of the resulting cilia. The material properties of the elastomeric polymer used directly affects the elastic modulus of the cilia. For a high sensitivity sensor, a polymer with low elastic modulus should be chosen. The polymer chosen for this work was Kraton D1163P, which is a linear poly(styrene-*b*-isoprene-*b*-styrene) triblock copolymer with tensile strength 10,3 MPa of and 300% modulus of 483 kPa. The cobalt particles used had an average particle size of 800 nm (OM Group Kokkola Finland).

Cilia sample was fabricated by following the general recipe described in [10]. A magnetic suspension consisting of 30 mg of cobalt particles and 30 mg of elastomeric polymer dissolved into 7.5 ml of toluene was prepared. The resulting suspension was ultrasonicated two times for five minutes with a Branson Sonifier S-450 with microtip. Tip amplitude of 25% was used for both sonication rounds. After sonication, the suspension was vigorously stirred by hand. This procedure was found to further reduce the agglomeration of cobalt particles in the suspension, increasing the quality of produced fibers.

After the sonication, the suspension was poured into a deep PTFE evaporation dish. Prior to this, thin strips of 150 μm thick microscope glass slides were placed to the bottom of the dish to serve as growth platforms. The dish was placed under an electromagnet, where the toluene was allowed to completely evaporate. After the evaporation, the glass strips were cut out of the thin elastomeric polymer film formed on the bottom of the dish during the evaporation process. The resulting cilia are depicted in figure 2. SEM micrographs of a single cilium are presented in figs. 3 and 4.

Fig. 2. Side-view of an array of cilia obtained after evaporation of a polymer/particle suspension in presence of magnetic field. Scale bar 5 cm.

The locations where cilia will form during the evaporation can be controlled by using the previously mentioned glass slides. It was observed that cilia will form on the edges of these glass plates during the evaporation of toluene. This is particularly useful if multiple cilia are used in flow detection, as the row formation is achieved simply by cutting away

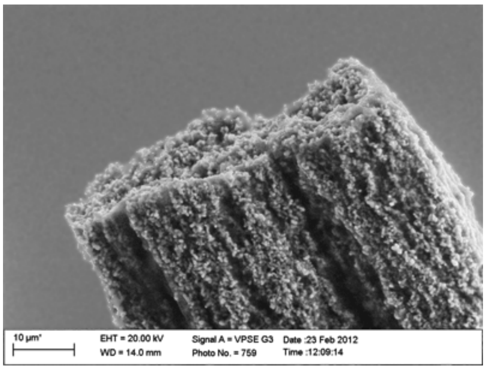

Fig. 3. ESEM (Carl Zeiss EVO HD) micrograph of cilium cross section. It is seen that the cobalt particles are distributed evenly throughout the fiber.

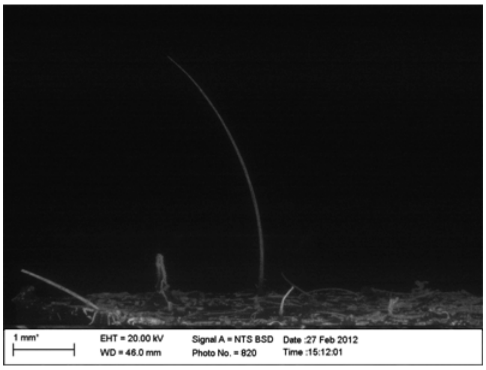

Fig. 4. Backscattered electron micrograph of a cilium. Other cilia on the substrate have been cut off with a knife. Cobalt as a heavy element gives more signal than the polymer, which can be seen on the substrate.

the extra cilia growing on top of the glass slide after the fabrication phase. Without the use of glass plates, the cilia seem to grow on completely random locations.

III. MODELING

A. Distributed dipole model for a single cilium

A model for the magnetic field of a cilium is needed to relate the deformation of the cilium and the magnetic flux density at the measurement point. Previously, a distributed multiple (DMP) approach has been used to characterize the magnetic field of a permanent magnet for sensing and actuating purposes [11], [12]. Finite element method (FEM) based models have been used to model the B-H-relation of magnetic microfiber bundles used in textiles for sensing and actuating purposes [13]. In order to obtain an accurate description of the cilium's magnetic field using finite element method, dense mesh is required. This is computationally considerably more expensive than using the DMP or similar method. Thus, the cilium is modelled as a spatially distributed set of magnetic dipoles, as presented in figure 5. The cilium is divided horizontally into n slices and each slice is modelled separately as a loop of k dipoles. The shape of the cilium is approximated as a right circular cone and thus the individual slices have the shape of circular cone frustum. The radius of the loop is determined by the average circumference of the slice.

The magnetic field of the cilium can then be calculated in the point of interest, P, with the location vector r by combining the magnetic fields of the dipoles. For each dipole, the magnetic field is calculated at point P, with the location vector $r_{i,j}$ in the dipole-centered coordinate system.

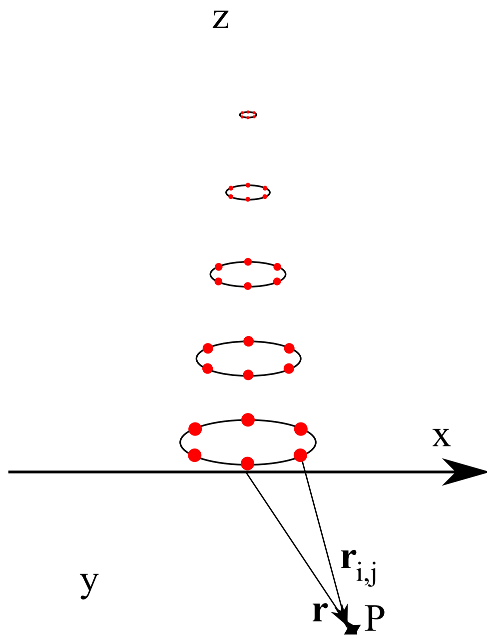

Fig. 5. Modeling cilium as a set of spatially distributed dipoles. The cilium is divided into n slices. Each slices is modelled as a loop of k dipoles.

The magnetic moment of the cilium, m_c, is calculated as presented in (1). Because of the assumed homogeneity of the cilium and the known proportion of cobalt and polymer in the solution, the magnetic moment of the cilium is calculated based on the volume of cobalt V_{Co} and polymer, V_p, in the cilium and magnetic moment per unit volume of cobalt M_{Co}. The magnetic moment per unit volume of cobalt is calculated based on the number of atoms in unit volume of cobalt, n_{Co} and the average magnetic moment of cobalt atom in bulk, $\bar{\mu}$. The magnetic moment is collinear to the surface normal of the cilium's base.

$$m_c = \frac{V_{Co}}{V_{Co}+V_p} V_c M_{Co} = \frac{V_{Co}}{V_{Co}+V_p} V_c n_{Co} \bar{\mu} \tag{1}$$

The magnetic moments of the dipoles are determined by the magnetic moment of the respective slice. The magnetic moment of a slice is proportional to the volume of the slice, V_s. The magnetic moment of a slice, m_s, is collinear to the magnetic moment of the cilium m_c.

$$m_s = \frac{V_s}{V_c} m_c \tag{2}$$

The strength of the dipole magnetic field in a point P outside the cilium, described by the vector $r^P = [x^P \; y^P \; z^P]$ can be calculated using the dipole term of the multipole expansion as presented in (3) [14].

$$B_d(r^P, m) = \frac{\mu_0}{4\pi \|r^P\|_2^3} 3 r_n^P (m \cdot r_n^P) - m, \tag{3}$$

where r_n^P denotes the normalized vector r^P. The strength of the field is characterized by the magnetic moment of the dipole, m.

The magnetic field contribution of a slice of cilium can thus be calculated by using (3) and (2):

$$B_s(r_s, m_s) = \sum_{j=1}^{k} B_d(r_j, \frac{m_s}{k}) \tag{4}$$

Furthermore, the magnetic field of the cilium can then be calculated by superposition of the magnetic fields of individual slices using (4), resulting in (5):

$$B_c(r,m) = \sum_{i=1}^{n} \sum_{j=1}^{k} B_d(r_{i,j}, \frac{m_i}{n}), \tag{5}$$

where $r_{i,j}$ is a vector pointing from the location of jth dipole of ith loop to the point of interest P. m_i denotes the magnetic moment of ith slice.

B. Parameter estimation

The magnetic field of the cilium was calculated using MATLAB. The model includes physical parameters, cilium height h_c, cilium base radius r_b, magnetic moment of the cilium m and the position of the cilium relative to the sensor location $p(x_f, y_f, z_f)$. In addition there are two modeling parameters, number of loops n and number of dipoles per loop k. These parameters will be estimated so that the model corresponds with experimental data. The estimation is done by measuring the magnetic flux density of the cilium's magnetic field in different positions respect to the base of the cilium. To simplify the measurement, this is done in a simple case of inclining a straight cilium relative to the magnetic field sensor, keeping the cilium base fixed and curvature of the cilium zero.

The estimation was done using Matlab Optimization Toolbox's Genetic Algorithm (GA). Genetic Algorithm is a probabilistic global optimization algorithm. Due to the probabilistic nature of the selected algorithm, the result of the algorithm slightly differs from run to run. Thus, multiple iterations are require to get a good estimate of the minimum of the search space.

The search space was bounded by introducing constraints to the physical parameters of the cilium. For cilium height h_c, base radius r_b and position $p_f = [x_f \; y_f \; z_f]$, the constraints were based on approximate manual measurements of the cilium. The modeling parameters (n,k) were constrained with an educated guess to avoid excess calculation. For the magnetic moment of cobalt m_{Co}, a textbook value was used [15].

The goal of the optimization is to minimize the quadratic cost function J subject to the parameter vector $v = [h_c, r_b, x_f, y_f, z_f n, l]$ (6), which essentially minimizes the sum of squared error of the model and the measurement points.

$$J = \operatorname*{argmin}_v \sum_i (B_{c,x}(v, \theta_i) - f(\theta_i)), \tag{6}$$

where $B_{c,x}(v,\theta_i)$ is the model's output for the x-component of the magnetic field (the value measured by the sensor) with parameters v and bending angle θ_i and $f(\theta_i)$ is the measured magnetic field with the corresponding angle.

IV. EXPERIMENTAL

A. Experimental setup

The experimental setup consisted of a magnetic field sensor, a sample holder, a data acquisition card and a digital camera with a macro lens. The experimental setup is illustrated in figure 6.

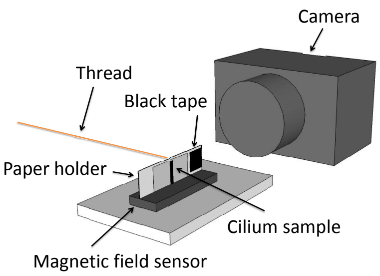

Fig. 6. Schematic view of the experimental setup. Single cilium is attached to a holder with transparent tape and the holder is placed on top of the magnetic field sensor. The cilium is tilted with a thread. Camera is used to measure the tilt angle of the cilium. Piece of shiny black electric tape is attached to holder to ease the angle measurement.

The magnetic field sensor used is a single axis magnetoresistive sensor with a Permalloy sensing element (Honeywell HMC1021Z). For sensitivity, the typical value of 1.0 $mV/V/Gauss$ was used. The sensor signal was amplified using a variable gain instrumentation amplifier and fed to a data acquisition card (National Instruments PCI-6033E). The data is read to computer via MATLAB.

A single cilium was carefully removed from the fabricated sample and rigidly attached to a holder with tape. The holder allows a straight cilium to be bent to an arbitrary angle without damaging the cilium while keeping the base of the cilium fixed. The cilium holder was placed on top of the magnetic field sensor so that the displacement of the cilium during bending is collinear to the direction of sensor's sensitive axis. The thickness of the sensor casing was measured to be 1.42 mm, so the distance between cilium's base and sensing element of the sensor was assumed to be 0.71 mm. The cilium was placed on top of the sensor case on the spot where the measured magnetic field is maximal by hand. It was observed that this point is unique, which enables deterministic placement of cilium to the same position in every measurement, within the limits of precision of the manual placement. Placement of the cilium sample was done manually to minimize the amount of magnetic mass in the vicinity of the sensor. The sample was then incrementally tilted by pulling the thread attached to the sample holder.

To measure the bending angle of the cilium, a digital camera (Canon EOS50D Digital SLR Camera with a Canon EF 100 mm f/2.8 USM macro lens) was used. The camera was placed so that the optical axis of the lens was perpendicular to the sensitive axis of the magnetic field sensor. A small piece of electrical tape was attached to the cilium holder to ease the measurement of the bending angle, as the flash of the camera then causes a thin reflection on the tape, which can be used to measure the bending angle. The bending angle of the cilium was measured manually from the camera images with the help of a custom MATLAB script, as illustrated in fig. 7.

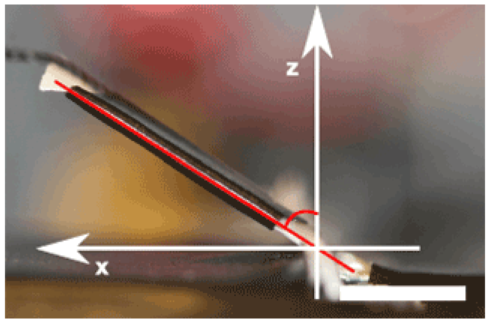

Fig. 7. The measurement of the tilt angle of the cilium. The angle is measured relative to the z-axis, which is normal to the sensitive axis of the magnetoresistive sensor. Scale bar 2 cm.

The magnetic field of the cilium was measured on 33 points, each corresponding to a different bending angle. A sensor bridge voltage of 7.5 V was used, resulting in sensitivity of 7.5 mV/Gauss. The measurement was done by recording 2000 data points with a 1 kHz sampling frequency for each angle and then averaging over the data points to remove the effects of measurement noise. During the measurement, no significant hysteresis between the bending angle and magnetometer reading was observed.

B. Experimental results

First, a polynomial was fit into the measurement data set to remove the DC bias. This DC bias originates from the external magnetic fields present during the measurement, e.g. magnetic field of earth and surrounding laboratory equipment.

The model was fit into the estimation data using the genetic optimization algorithm. The initial values based on rough measurements and the resulting optimized parameters for the cilium are presented in table I. The value of the cost function with the optimized parameters is $4.79604 \cdot 10^{-7} V^2$.

TABLE I
INITIAL AND OPTIMIZED PARAMETERS OF THE CILIUM

Parameter	Initial value	Optimized value
Height (mm)	3	3.2613
Base radius (mm)	0.25	0.1801
Position (x,y,z) (mm)	(0,0,0)	(1.4727,1.9891,0.3804)
Loops	6	2
Dipoles per loop	3	5

The optimized values for the parameters with measured initial values differ only slightly from the initial values. There is some deviation in the position of the cilium compared to the initial value, which was found by maximizing the sensor reading with zero bending angle. This deviation may be because of errors in the manual positioning and fixing of the cilium holder and due to the scale of the cilium and the sensing element being near each other. Other possible error sources are the assumed cylindrical shape of the cilium and spatial distribution of the cobalt particles in the cilium being not completely homogeneous. Furthermore, the assumption of volumetric fractions of cobalt and polymer in the cilia might not be as assumed.

The measured data, initial model and the optimized model are presented in fig. 8. The model calculated using the initial parameters somehow describe the magnetic field of the cilium with angles smaller than 40 degrees, but after that fails completely. The optimized model corresponds to the measurement data well on the whole range.

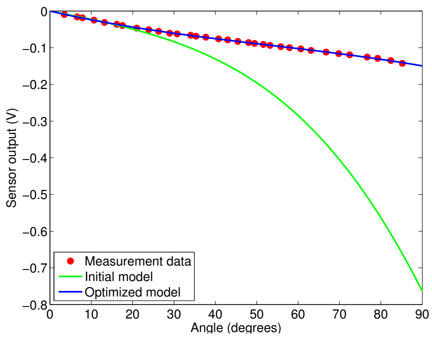

Fig. 8. Measured data points, model corresponding to the initial measurements and the model with estimated parameters.

C. Model sensitivity analysis

The sensitivity of the model to parameter variations was analysed with respect each parameter separately when holding other parameters constant at their optimized values. The results of the analysis are illustrated in figs. 9-12.

The sensitivity analysis of cilium's coordinates are presented in figs. 9 and 10. The x-coordinate of the cilium is the most sensitive parameter in the model. This also implicates that in order for the model to capture the magnetic field of the cilium, the model must be calibrated by the parameter optimization method. It can also be seen from fig. 9 that the model is relatively tolerant to errors in the y-coordinate of the cilium. The error is also symmetric relative to y-axis. The model is tolerant to errors in the z-coordinate of the cilium, as seen from fig. 10. The calculated model sensitivity to spatial coordinates of the cilium imply that for multiple cilium arrays, it is required that the fabrication process allows position-wise deterministic growing of cilia.

The effects of the two modeling parameters, number of loops used to model the cilium, n and number of dipoles per loop, k, are illustrated in fig. 11. Number of dipoles per loop has only little impact to the modeling results whereas the number of loops clearly affects the model accuracy.

Figure 12 illustrates the sensitivity of the model to variations in cilium height and cilium base diameter d. The figure indicates that the model is more sensitive to errors in

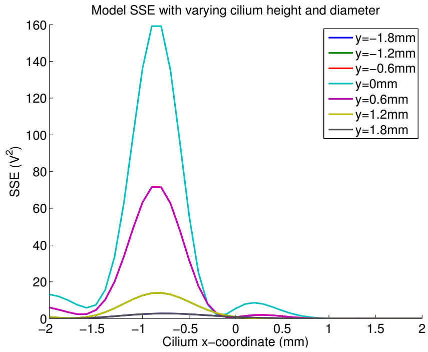

Fig. 9. Model sensitivity to errors in x and y coordinates

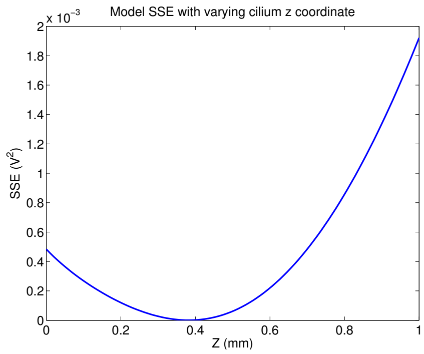

Fig. 10. Model sensitivity to errors in the z coordinate of the cilium

the cilium diameter than in cilium height. This is expected because of the rapid attenuation of magnetic field over distances and the geometrical shape of the cilium, where most of the magnetic mass is located near the base of the cilium.

V. DISCUSSION

The proposed model for characterization of the magnetic field of a cilium contains in total seven parameters, two of those being modeling parameters. The sensitivity analysis of the model suggests that the location of the cilium relative to the magnetic field sensor is the most critical parameter in the model. Small errors in cilium's position on the sensitive axis of the sensor can lead to situations where the model

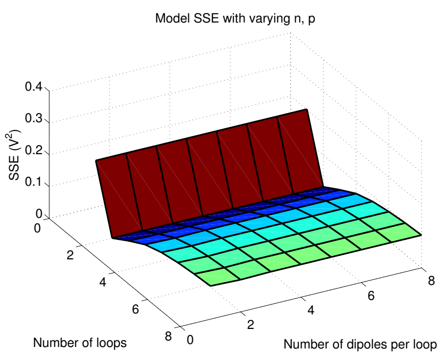

Fig. 11. Model sensitivity to modeling parameters, i.e. the number of loops and the number of dipoles per loop.

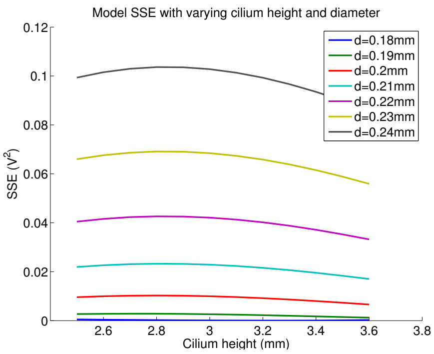

Fig. 12. Model sensitivity to inaccuracies in cilium bottom diameter and height.

completely fails to describe the magnetic field of the cilium. This leads to a need of calibration procedure for the sensor to estimate the parameters of the model.

The calibration procedure involves measurements of the magnetic field of the cilium in multiple points. In the experiment conducted in this paper, the magnetic field was measured in 33 points near the base of the cilium, which was more than enough to calibrate the model. The number of points could be reduced, as long as the calibration data contains measurements from variety of locations.

The model for the magnetic field of the cilium is computationally expensive regarding sensor performance. From fig. 8 it can be seen that once the parameters of the model are estimated, the model can be reasonably well approximated with a piece-wise linear function with two corner points. Furthermore, the approximating function can be reduced to a linear polynomial if the range of bending angles is reduced. However, it must be kept in mind that the shape of the magnetic field curve is location dependant. Thus, the model must be first used to characterize the magnetic field before any polynomial approximations can be made.

In this work, the cilia were inspected as single-axis sensors. Biaxial sensing would require a biaxial magnetic force sensor. Due to the small size of the cilium, the two sensing elements of the sensor would need to be located in close proximity of each other in order for the magnetic field of the cilium be strong enough to be detected. In practice this might be difficult to achieve.

The cilia used in this work have previously been demonstrated as actuators for particle transport and mixing of liquids [10]. With this in mind, question for simultaneous sensing and actuation arises. In simultaneous actuation and sensing, the actuating magnetic field and the magnetic field of the cilium would be superimposed in the measurement of the magnetic field sensor. Thus, the actuating field would need to be compensated to obtain valid measurement for the cilium. The main difficulty is accurate compensation of the actuating field taking into account the magnitude difference of the actuating field and the magnetic field of the cilium.

As a conclusion, we have proposed a mathematical model based on the concept of magnetic dipole to estimate the magnetic field of a cilium containing magnetic microparticles that can be used to estimate geometric deformation of a cilium, enabling the use of such cilium in force sensing. The cilia are fabricated in a template-free way, which is simple and inexpensive compared to previously suggested fabrication methods.

The proposed model is sensitive to errors in the location of the cilium relative to the sensing element and requires a calibration procedure involving measurements of the magnetic field of the cilium in multiple points. Once calibrated, the model accurately describes the magnetic field of the cilium. Further work is needed to improve the model to make it less sensitive to parameter variations and to investigate whether the calibration procedure could be omitted.

References

[1] W. A. Abou Alaiwi, S. T. Lo, and S. M. Nauli, "Primary Cilia: Highly Sophisticated Biological Sensors," *Sensors*, vol. 9, no. 9, pp. 7003–7020, 2009.

[2] A. Dagamseh, C. Bruinink, H. Droogendijk, R. Wiegerink, T. Lammerink, and G. Krijnen, "Engineering of Biomimetic Hair-Flow Sensor Arrays Dedicated to High-Resolution Flow Field Measurements," in *IEEE Sensors 2010 Conference*. IEEE, 2010, pp. 2251–2254.

[3] F. Fahrni, M. W. J. Prins, and L. J. van IJzendoorn, "Micro-fluidic actuation using magnetic artificial cilia," *Lab Chip*, vol. 9, pp. 3413–3421, 2009.

[4] G. Kokot, M. Vilfan, N. Osterman, A. Vilfan, B. Kavcic, I. Poberaj, and D. Babic, "Measurement of fluid flow generated by artificial cilia," *Biomicrofluidics*, vol. 5, no. 3, p. 34103, 2011.

[5] A. Dagamseh, C. Bruinink, M. Kolster, R. Wiegerink, T. Lammerink, and G. Krijnen, "Array of biomimetic hair sensor dedicated for flow pattern recognition," in *Design Test Integration and Packaging of MEMS/MOEMS (DTIP), 2010 Symposium on*. IEEE, 2010, pp. 48–50.

[6] Z. Fan, J. Chen, D. B. J.Zou, C.Liu, and F.Delcomyn, "Design and fabrication of artificial lateral line flow sensors," *AIP Journal of Micromechanics and Microengineering*, vol. 12, no. 5, pp. 655–661, June 2002.

[7] N. Izadi, R. Jaganatharaja, J. Floris, and G. Krijnen, "Optimization of Cricket-inspired, biomimetic artificial hair sensors for flow sensing," *Arxiv preprint arXiv:0802.3768*, no. April, pp. 25–27, 2008.

[8] N. Chen, C. Tucker, J. M. Engel, Y. Yang, S. Pandya, and C. Liu, "Design and Characterization of Artificial Haircell Sensor for Flow Sensing With Ultrahigh Velocity and Angular Sensitivity," *October*, vol. 16, no. 5, pp. 999–1014, 2007.

[9] F. Li, W. Liu, C. Stefanini, X. Fu, and P. Dario, "A Novel Bioinspired PVDF Micro/Nano Hair Receptor for a Robot Sensing System." *Sensors (Basel, Switzerland)*, vol. 10, no. 1, pp. 994–1011, Jan. 2010.

[10] J. V. I. Timonen, C. Johans, K. Kontturi, A. Walther, O. Ikkala, and R. H. A. Ras, "A facile template-free approach to magnetodriven, multifunctional artificial cilia." *ACS Applied Materials & Interfaces*, vol. 2, no. 8, pp. 2226–30, Aug. 2010.

[11] H. Son and K.-M. Lee, "Distributed Multipole Models for Design and Control of PM Actuators and Sensors," *IEEE/ASME Transactions on Mechatronics*, vol. 13, no. 2, pp. 228–238, Apr. 2008.

[12] W. Fang and H. Son, "Optimization of Measuring Magnetic Fields for Position and Orientation Tracking," *IEEE/ASME Transactions on Mechatronics*, vol. 16, no. 3, pp. 440–448, June 2011.

[13] S. Wiak, A. Firych-Nowacka, and K. Smolka, "Computer model of 3-D magnetic micro fibres used in textile actuators," in *2008 18th International Conference on Electrical Machines*, vol. i. IEEE, Sept. 2008, pp. 1–6.

[14] D. J. Griffiths, "An Introduction to Electrodynamics: From the Standpoint of the Electron Theory," *Nature*, vol. 110, no. 2763, pp. 509–509, Oct. 1922.

[15] N. W. Ashcroft and N. D. Mermin, *Solid State Physics*, ser. Holt-Saunders International Editions: Science : Physics, F. Seitz and D. Turnbull, Eds. Holt, Rinehart and Winston, 1976, vol. 2, no. ISBN 0-471-92805-4.